

dr inż. Andrzej Gołdasz, agoldasz@metal.agh.edu.pl

prof. dr hab. inż. Zbigniew Malinowski, malinows@metal.agh.edu.pl

dr inż. Beata Hadała, bhadala@metal.agh.edu.pl

STUDY OF HEAT BALANCE IN THE ROLLING PROCESS OF BARS

Summary

Hot rolling of shapes is one of metal forming processes that is most difficult to finite element modeling. Temperature computation is an important part of finite element software and has great influence on the solution accuracy. Computed temperature fields are generally qualitatively correct and it is not easy to eliminate wrong results. One of the possibilities to validate the temperature field is heat balance calculation in the control volume. Temperature computation is generally based on an approximate solution to the heat transport equation. Typical way of verification of the solution accuracy is to compare results of computation to measurements. However, it is not always possible or acceptable due to experimental costs. Another possibility of verification gives heat balance calculation in the control volume for separate stages of rolling. Two and three dimensional models of heat transfer in rolling processes have been tested. Stability of temperature field computation and fulfillment of heat balance have been studied for bar cooling in air and rolling between flat rolls for two sets of boundary conditions. The two dimensional model gives the temperature only in the cross section of the rolled material. Three dimensional temperature field is obtained by moving the cross section into the rolling direction. The three dimensional model uses steady solution to the heat transfer in the control volume.

Introduction

The finite element method gives a possibility to compute temperature of the rolled material at element nodes based on the solution to a linear set of equations. The problem can be treated as a steady one since there is no the bar temperature change in time and can be well described by the convection-diffusion heat transfer equation. Several methods can be used to linearise the heat transport equation. However, in the case of convection dominated processes oscillatory solution are observed and convergence is not obvious. Several methods have been

proposed to overcome these difficulties. One of the most popular formulations uses non-symmetric weighting functions instead of linear shape functions. The method is efficient but in some cases solutions to the temperature field are not satisfactory. Transient or iterative methods can be successfully employed but the computation time is generally high in the case of three-dimensional problems. Detailed descriptions of the numerical methods can be found in [10]. The internal heat source in the convection-diffusion heat transport equation resulting from the work of plastic deformation makes the solution much more complicated. Two and three-dimensional models can be employed to compute a temperature field in bar rolling processes [3], [8], [10]. Steady and transient formulations are possible. Steady solutions reduce significantly the computation time [4], [5]. However, even steady solutions require some iterations in order to correct the material shape and properties. Interaction between the deformation field and temperature may lead to several iterations in order to complete the thermal-mechanical model. In this case a transient solution can be more accurate and efficient [4]. However, stable and good-looking results may not be accurate. It makes the interpretation of the temperature computation very difficult. It is not possible to validate the temperature field each time by measurement. In the paper a method of validation based on the heat balance in the control volume has been proposed. Transient two-dimensional model and steady three-dimensional solution have been compared. Accuracy of the solutions for bar cooling in air and rolling between flat dies has been tested for two sets of boundary conditions.

Heat transfer model

In the case of **3D finite element model** the bar temperature field is computed from the solution to the steady heat transfer equation [9]:

$$\frac{\partial T}{\partial \tau} + v_x \frac{\partial T}{\partial x} + v_y \frac{\partial T}{\partial y} + v_z \frac{\partial T}{\partial z} = \frac{\lambda}{\rho c} \left(\frac{\partial^2 T}{\partial x^2} + \frac{\partial^2 T}{\partial y^2} + \frac{\partial^2 T}{\partial z^2} \right) + \frac{q_v}{\rho c} \quad (1)$$

where:

T – temperature, K,

τ – time, s,

v_x, v_y, v_z – velocity field, m/s,

λ – thermal conductivity, W/(m K),

q_v – internal heat source, W/m^3 ,

c – specific heat, $\text{J}/(\text{kg K})$,

ρ – density, kg/m^3 .

Eq. (1) describes the energy balance of a bar moving through the control volume where the internal heat source q_v represents the heat of phase change and the plastic work dissipation:

$$q_v = Q_{\gamma\alpha} \frac{V_\gamma - V_\gamma^o}{\Delta\tau} + \sigma_p \dot{\epsilon}_i \left(1 - \frac{20H'}{E} \right) \quad (2)$$

where:

$Q_{\gamma\alpha}$ – heat of phase change, J/m^3 ;

V_γ, V_γ^o – phase fraction at time $\tau = \tau - \Delta\tau$ and $\tau = \tau_o$, respectively,

E – Young's modulus, Pa,

$\dot{\epsilon}_i$ – effective rate of deformation, $1/\text{s}$,

H' – elastoplastic hardening modulus, Pa,

σ_p – flow stress, Pa.

Flow stress as a function of temperature, effective rate of deformation and effective strain has been calculated from Shida equation [7]. The phase fraction V_γ as a function of the transformation start temperature T_s and the transformation end temperature T_f can be determined from [3]:

$$V_\gamma = 1 - \exp\left(K_{sf} \frac{T_s - T}{T_f - T_s} \right) \quad (3)$$

In Eq. (3) K_{sf} is a constant with the value between 2 and 10.

Solution to the general heat transfer Eq. (1) should obey the boundary conditions specified on the bar surface S :

$$q = \alpha (T_m - T_a) \quad (4)$$

where:

α – combined heat transfer coefficient, $\text{W}/(\text{m}^2 \text{K})$,

T_m – bar surface temperature, K,

T_a – ambient temperature, K.

The bar loses heat to surroundings by radiation and convection. The radiation heat transfer coefficient α_r can be calculated from:

$$\alpha_r = 5.67 \cdot 10^{-8} \varepsilon_m \frac{T_m^4 - T_a^4}{T_m - T_a} \quad (5)$$

where:

ε_m – emissivity of the bar surface.

Interface between bar and roll can be characterized by thermal contact conductance and the value of the heat transfer coefficient α_p is expressed by the empirical equation:

$$\alpha_p = 36400 - 74 t_m + 0,04 t_m^2 \quad (6)$$

where:

t_m – bar surface temperature, °C.

Convection heat transfer coefficient α_c may vary from 10 to 250 W/(m² K). The Nusselt relation [9] can be used to calculate α_c for air cooling:

- Laminar flow:

$$Nu = 0,664 Re^{0,5} Pr^{1/3} \varepsilon_T \quad (7)$$

- Intermediate and turbulent flow:

$$Nu = 0,037 Re^{0,8} Pr^{1/3} \varepsilon_T \quad (8)$$

The Reynolds number Re and the Prandtl number Pr should be evaluated at the air bulk average temperature. The coefficient ε_T takes into account the influence of the bar surface temperature on the air temperature in the boundary layer:

$$\varepsilon_T = \left(\frac{Pr}{Pr_m} \right)^{0,19} \quad (9)$$

The subscript m indicates that the Prandtl number Pr is to be calculated at the bar surface temperature. Thermal conductivity, specific heat and density are calculated as function of temperature depending on the material chemical composition.

The Galerkin method [10] has been employed to solve Eq. (1). It has led to the set of linear equations:

$$(K_{nn} + W_{nn})T_n = G_n \quad (10)$$

where: n is number of unknowns and T_n are unknown temperatures at element nodes. Several formulations depending on the choice of the weighting and shape functions can be used to

define the matrices K_{nm} , W_{nm} and vector G_n . In the present study the domain V is divided into 8 node elements with linear weighting and shape functions. It gives for one element:

$$W_{ij} = \sum_{k=1}^8 \varrho^k c^k \left(v_x^k N_i \frac{\partial N_j}{\partial x} + v_y^k N_i \frac{\partial N_j}{\partial y} + v_z^k N_i \frac{\partial N_j}{\partial z} \right) D_V^k \quad (11)$$

$$K_{ij} = \sum_{k=1}^8 \lambda^k \left(\frac{\partial N_i}{\partial x} \frac{\partial N_j}{\partial x} + \frac{\partial N_i}{\partial y} \frac{\partial N_j}{\partial y} + \frac{\partial N_i}{\partial z} \frac{\partial N_j}{\partial z} \right) D_V^k + \sum_{s=1}^8 L^s \sum_{k=1}^4 N_i N_j \alpha^k D_S^k \quad (12)$$

$$G_i = \sum_{k=1}^8 q_V^k N_i D_V^k + \sum_{s=1}^6 L^s \sum_{k=1}^4 N_i (\alpha^k T_a^k - q^k) D_S^k \quad i = 1, \dots, 8; \quad j = 1, \dots, 8 \quad (13)$$

where:

N_i – linear shape functions,

k – Gaussian integration point number,

D_V – constant resulting from Gaussian quadrature formula and volume element coordinates transformation to a prism region,

D_S – constant resulting from Gaussian quadrature formula and surface element coordinates transformation to a square region,

L^s – constant equal 0 or 1 if on element surface boundary conditions are specified.

The unknown parameters T_n in Eq. (10) resulting from this formulation are temperature values in element nodes, Table 1. Gaussian elimination scheme is used to solve band diagonal system of linear equations (10).

The **2D finite element model** is the transient solution to the heat transfer in the bar cross section :

$$\lambda \left(\frac{\partial^2 T}{\partial x^2} + \frac{\partial^2 T}{\partial y^2} \right) + q_v - \varrho c \frac{\partial T}{\partial \tau} = 0 \quad (14)$$

Three dimensional temperature field is obtained by moving the cross section from entry to exit of the control volume as shown in Fig. 1.

The boundary conditions on the bar surface are specified in the same way as for the 3D model.

The Galerkin method employed to Eq. (10) over the time period $\Delta\tau \in (\tau, \tau+\Delta\tau)$ gives the set of linear equations:

$$A_{ij}(\tau)T_j(\tau + \Delta\tau) = B_i(\tau) \quad (15)$$

where:

$$A_{ij}(\tau) = \frac{1}{3} [K_{ij}(\tau)] + \frac{1}{2\Delta\tau} C_{ij}(\tau)$$

$$B_i(\tau) = \left[-\frac{1}{6} (K_{ij}(\tau)) + \frac{1}{2\Delta\tau} C_{ij}(\tau) \right] T_i(\tau) + \frac{1}{6} G_i(\tau) + \frac{1}{3} G_i(\tau + \Delta\tau)$$

$$G_i = \sum_{k=1}^2 L_k N_i \alpha^k T_a^k D_f^k + \sum_{k=1}^4 N_i q_V^k D_k$$

$$C_{ij} = \sum_{k=1}^4 N_i N_j \rho^k c^k D^k$$

$$K_{ij} = \sum_{k=1}^4 \lambda^k \left(\frac{\partial N_i}{\partial x} \frac{\partial N_j}{\partial x} + \frac{\partial N_i}{\partial y} \frac{\partial N_j}{\partial y} \right) D^k + \sum_{k=1}^2 \alpha^k L^k N_i N_j D^k$$

Mechanical model

The three dimensional flow of a material through the control volume V is considered. The problem is formulated in the spatial reference frame. The material's constitutive relation in the plastic region is governed by the Levy - Mises flow equations

$$s_{ij} = \frac{2}{3} \frac{\sigma_i}{\dot{\epsilon}_i} d'_{ij} \quad (16)$$

where:

σ_i – effective stress, Pa,

$\dot{\epsilon}_i$ – effective rate of deformation, 1/s,

d'_{ij} – deviator of the rate of deformation tensor.

Application of the principle of the virtual velocities to the deformation power under the assumption that the elastic work is dissipative yields the functional:

$$\Psi(v_i) = \int_V \left[\sigma_p \dot{\epsilon}_i + \frac{\Delta\tau H'}{2} \dot{\epsilon}_i^2 \right] dV + \int_V \frac{\Delta\tau E}{6(1-2\nu)} d_{kk}^2 dV + \int_S \tau_s |v| dS \quad (17)$$

where:

d_{kk} – rate of the volume change,

H' – elastoplastic hardening modulus, Pa

σ_p – flow stress of the rolled material, Pa

ν – function defining Poisson's ratio,

$\Delta\tau$ – time increment, s,

τ_s – friction stress specified on S , Pa,

$|v|$ – velocity discontinuity on S , m/s .

The first term in Eq. (17) represents the deformation power given by the product of the deviator of the Cauchy stress tensor s_{ij} and the deviator of the rate of deformation tensor d'_{ij} at the end of time increment $\Delta\tau$. The incompressibility condition on the velocity field v_i can be enforced by the Lagrange multiplier method [1] or the penalty function method [2]. In the developed model the material deformed is assumed to be near incompressible and the penalty function:

$$\Psi = \frac{\Delta\tau E}{6(1-2\nu)} d_{kk}^2 \quad (18)$$

has been used. The power of volume change is dissipative and the the Poisson's ratio is assumed to be a continuous material function [6]:

- for $\sigma_i \leq \sigma_l$

$$\nu = \nu_o \quad (19)$$

- for $\sigma_i > \sigma_l$

$$\nu = \nu_{max} - (\nu_{max} - \nu_o) \exp\left[1 - \beta \frac{\sigma_i}{\sigma_l}\right] \quad (20)$$

where:

ν_{max} – maximum value of the Poisson's ratio,

ν_o – minimum value of the Poisson's ratio,

β – scaling factor,

σ_l – proportionality limit of the deformed material, Pa.

The maximum value of the Poisson's ratio is 0.5 for fully developed plastic flow, and the minimum value is near 0.35 typical for elastic deformation of steel. Cauchy stress tensor can be calculated from:

$$\sigma_{ij} = s_{ij} + \delta_{ij} \sigma_m \quad (21)$$

In Eq. (21) δ_{ij} is the Kronecker delta, and the mean stress σ_m is given by:

$$\sigma_m = \frac{E}{3(1-2\nu)} (d_{xx} + d_{yy} + d_{zz}) \quad (22)$$

The last integral in Eq. (17) introduces the friction power on the material - rolls contact surface. The friction factor m is used to calculate the friction stress:

$$\tau_s = \frac{m \sigma_p}{\sqrt{3}} \quad (23)$$

Friction factor can vary from 0 to 1. For hot rolling of bars friction factor $m=0.5$ is used in computations. The steady formulation of the mechanical model in the Eulerian reference frame enables the boundary conditions to be satisfied globally in the final configuration and reduces greatly the computations time.

Results of heat balance computations

The developed 2D and 3D models of the bar temperature field has been used to calculate the discrepancy of heat balance in the control volume V . For the control volume shown in Fig. 1 the discrepancy in heat balance can be calculated from:

$$\dot{Q}_{inp} + \dot{Q}_{out} + \dot{Q}_a = \Delta Q \quad (24)$$

where:

ΔQ – discrepancy in heat balance, W;

$\dot{Q}_{inp} = \int_S \rho c v_{inp} T dS$ – heat flux at entry to the control volume, W,

$\dot{Q}_{out} = \int_S \rho c v_{out} T dS$ – heat flux at exit from the control volume, W,

$\dot{Q}_a = \int_S q dS$ – heat loses to surroundings, W;

S – side surface of the bar, m^2 ;

v_{inp} – velocity normal to the entry plane of the control volume, m/s.

v_{out} – velocity normal to the exit plane from the control volume, m/s.

Five computation tests have been carried out. Test no 1, 2, 3 and 4 concern cooling of a bar moving with constant speed in air. The initial bar temperature was 1100°C . Bar dimensions in the cross section are $0,175\text{m} \times 0,260\text{m}$. The bar length is 0.5m . In the case of test no 1 the bar has been cooled in air. Heat flux $q = 2 \cdot 10^5 \text{ W/m}^2$ has been specified on the bar surface. Transient 2D finite element model has been used to solve the problem. In the case of test no 2 steady 3D solution has been employed. Constant heat flux boundary condition has been changed to convective heat transfer in the case of test no 3 and 4. Combined heat transfer coefficient $\alpha = 150 \text{ W/(m}^2 \text{ K)}$ has been specified on the bar surface. Transient 2D model has been used to compute the temperature field in test no 3. In the case of test no 4 3D steady model has been used. Tests 5, 6 and 7 concern temperature drops during bar rolling between flat rolls. In order to simplify the heat transfer problem internal heat generation due to plastic work and phase transformation have been neglected. Test no 5 is steady 3D solution and tests 6 and 7 are 2D transient solutions. Convective boundary conditions $\alpha = 150 \text{ W/(m}^2 \text{ K)}$

have been specified on the bar surface in tests 5, 6 and 7. Heat losses to the rolls have been taken into account as well.

The transient 2D model and steady 3D model have given almost identical temperature distribution on the bar surface cooled in air. Only 2°C difference in bar surface temperature has been noted, Fig. 2. Heat balance in the control volume has been satisfied very well, Fig. 3, and errors do not exceeded 0.01% of the heat flux at the entry to the control volume, Fig. 4. The heat balance errors for all tests have been shown in table 2.

It can be seen that in the case of bar cooling all methods have given very accurate results regardless of the type of boundary conditions on the bar surface. Bar deformation has changed the solution accuracy radically. In Fig. 5 the temperature variation on the bar surface has been shown. Steady 3D solution has given oscillatory solution to the temperature field and the heat balance error has reached 49 MW, Fig. 6, which is almost 7% of the heat flux value at entry to the deformation zone. Transient 2D solution is much more accurate and gives reasonable temperature variation on the bar surface. However, the heat balance error is 5%, Fig. 7. Finite element mesh refinement has improved the heat balance by 1%.

Conclusions

Accuracy of the finite element solution to the temperature field of the bar moving in air and rolled between flat rolls has been analyzed. Two dimensional transient solution and three dimensional steady formulation have been compared. Constant heat flux and convective type of boundary conditions has been prescribed on the bar side surface. In the case of bar moving in air all methods have given very accurate results. The shape change of the bar due to plastic deformation has large influence on stability of steady 3D solution. The velocity gradients has caused the oscillatory temperature variation on the bar surface in case of steady formulation. Two dimensional transient formulation is very efficient and has given the best results in all cases. Finite element mesh refinement in the bar cross section leads to improvement of the heat balance in the control volume.

Table 1. Chemical composition and thermal properties of steel used in computations.

Chemical composition	C=0,4÷0,75; Mn=0,6÷2,1; Si<0,5; P<0,005, S<0,005	%
Specific heat	$c = 486,522 + 161,004(T - 273,15) + 418,014(T - 273,15)^2$, dla $T < T_s$ $c = 647,221 + 5,852(T - 273,15)$, dla $T > T_f$ $c = c_1 + (c_2 - c_1) \frac{T-T_s}{T_f-T_s}$, dla $T_s < T < T_f$ $c_1 = 486,522 + 161,004(T - 273,15) + 418,014(T - 273,15)^2$ $c_2 = 647,221 + 5,852(T - 273,15)$	J/(kg·K)
Heat conduction coefficient	$\lambda = 42 - 16(T - 273,15)$, dla $T < T_s$ $\lambda = 11,9 + 5,64t$, dla $T > T_f$ $\lambda = \lambda_1 + (\lambda_2 - \lambda_1) \frac{T-T_s}{T_f-T_s}$, dla $T_s < T < T_f$ $\lambda_1 = 42 - 16(T - 273,15)$ $\lambda_2 = 11,9 + 5,64(T - 273,15)$	W/(m·K)
Density	$\rho = \frac{7850}{1 + 0,0002(T - 273,15)^3}$	kg/m ³

Table 2. Heat balance discrepancy for the bar cooling and rolling tests.

Test No	1	2	3	4	5	6	7
ΔQ [kW]	-87,87	-3,14	-66,83	0,27	49761,94	32716,15	28475,79
$\frac{ \Delta Q }{Q_{inp}}$ [%]	0,01	0,00	0,01	0	6,88	4,57	3,93

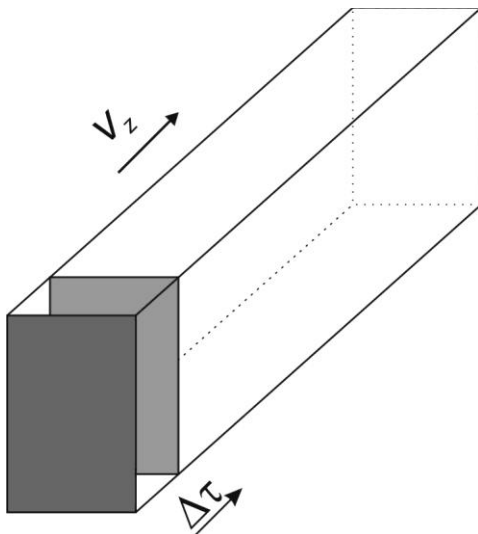


Figure 1. Scheme of 2D transient solution of the heat transfer in the bar cross section.

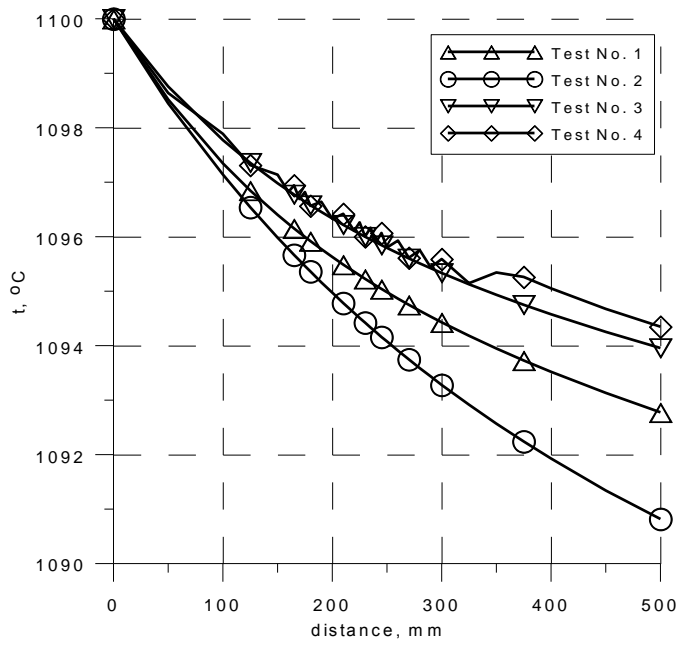


Figure. 2. Temperature variation on the billet surface cooled in air.

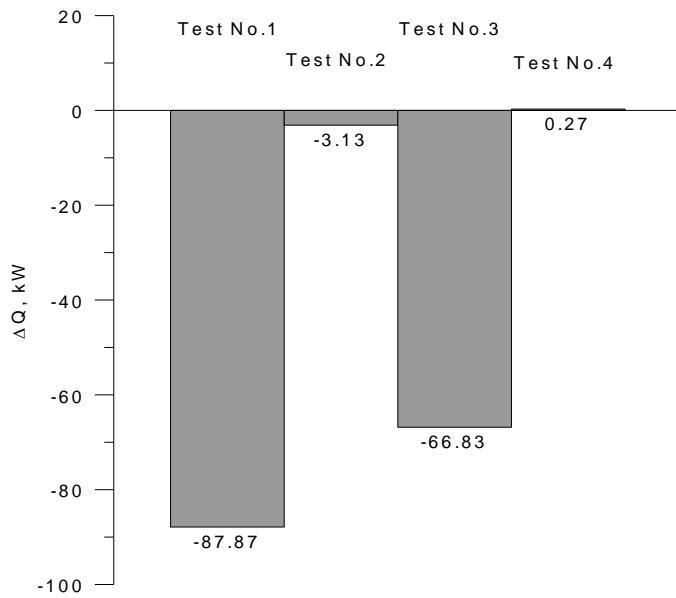


Figure. 3. Discrepancy of the heat balance for bar cooling in air.

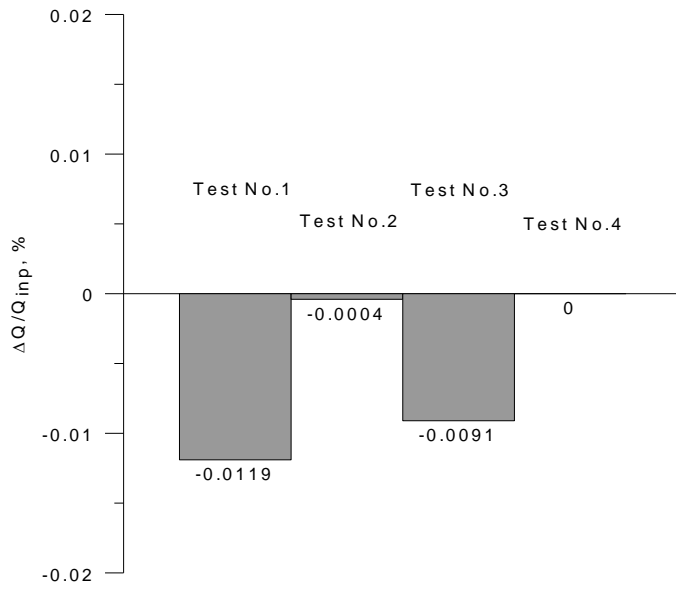


Figure 4. Discrepancy of the heat balance for bar cooling in air in percent of the heat flux at entry to the control volume.

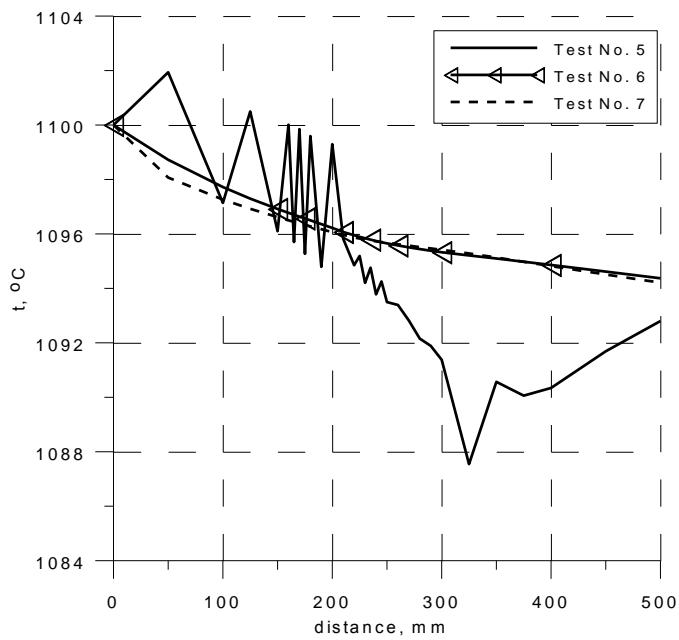


Figure 5. Temperature variation on the rolled billet surface.

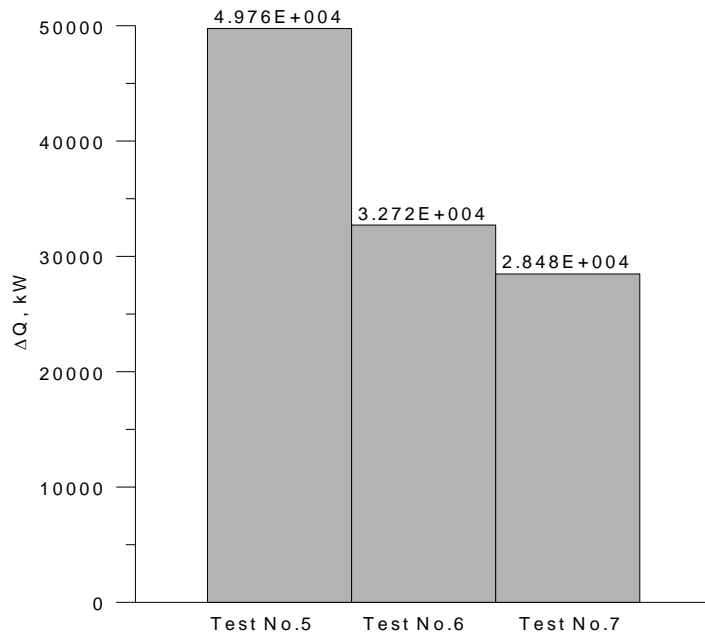


Figure 6. Discrepancy of the heat balance for bar bar rolling between flat rolls.

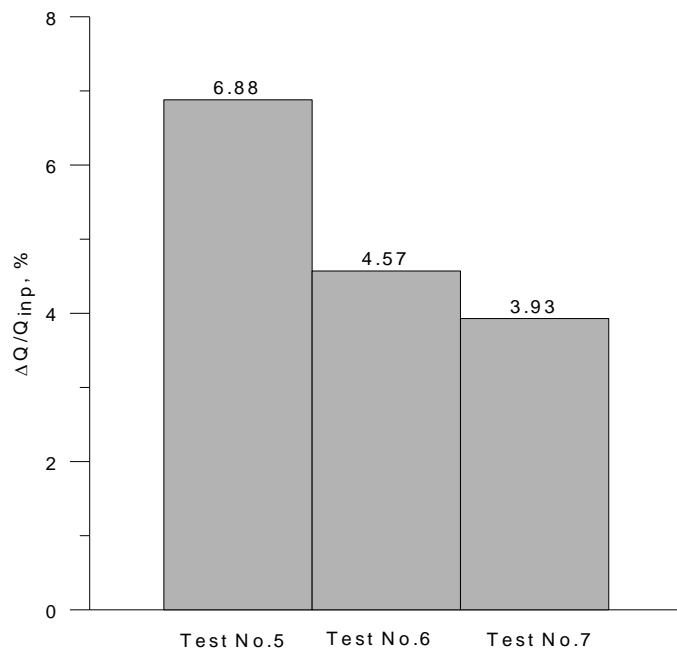


Figure 7. Discrepancy of the heat balance for bar bar rolling between flat rolls in percent of the heat flux at entry to the control volume.

Literature

1. Kręglewski T., Rogowski T., Ruszczyński A., Szymanowski J.; *Metody optymalizacji w języku FORTRAN*; PWN, Warszawa (1984).
2. Lee C.H. and Kobayashi S.; *New solution to rigid-plastic deformation problems using a matrix method*; *Trans. ASME, J. Engrg. Ind.*, vol. 95, 865-871 (1973).
3. Malinowski Z.; *Numeryczne modele w przeróbce plastycznej i wymianie ciepła*; AGH Uczelniane Wydawnictwa Naukowo-Dydaktyczne, Kraków (2005).
4. Malinowski Z.; *Stabilizacja algorytmu MES w rozwiązaniach zagadnienia przewodzenia ciepła w warunkach konwekcji ze źródłem ciepła*; *Informatyka w Technologii Materiałów*, vol. 1, no. 3-4, 135-146 (2001).
5. Malinowski Z., Gołdasz A., Hadała B., Banach M., Zygmunt T.; *Modelowanie numeryczne pól temperatury kształtowników walcowanych na gorąco*; *Hutnik Wiadomości Hutnicze*, no. 4, 176-181 (2008).
6. Malinowski Z., Lenard J.G.; *Experimental substantiation of an elastoplastic finite element scheme for flat rolling*; *Comp. Methods. Appl. Mech. and Engrg.*, vol. 104, 1-17 (1993).
7. Murthy A., Lenard J.G.; *Statistical Evaluation of Some Hot Rolling Theories*; *Journal of Engineering Materials and Technology*, vol. 104, no. 1, 47-52 (1982).
8. Pietrzyk M., Lenard J.G.; *Thermal-Mechanical Modelling of the Flat Rolling Process*; Springer-Verlag Berlin, Heidelberg (1991).
9. Wiśniewski S., Wiśniewski T.S.; *Wymiana ciepła*; WNT Warszawa (1997).
10. Zienkiewicz, O.C. and Taylor, R.L.; *The Finite Element Method, Vol. 1: The Basis*; fifth ed. Butterworth-Heinemann, Oxford (2000).

The work was financed by The Ministry of Science and Higher Education.

Projects No R07 0008 04/2008 and No N508 002 32/0158

Table 1. Chemical composition and thermal properties of steel used in computations.

Table 2. Heat balance discrepancy for the bar cooling and rolling tests.

Figure 1. Scheme of 2D transient solution of the heat transfer in the bar cross section.

Figure. 2. Temperature variation on the billet surface cooled in air.

Figure. 3. Discrepancy of the heat balance for bar cooling in air.

Figure. 4. Discrepancy of the heat balance for bar cooling in air in percent of the heat flux at entry to the control volume.

Figure 5. Temperature variation on the rolled billet surface.

Figure 6. Discrepancy of the heat balance for bar rolling between flat rolls.

Figure 7. Discrepancy of the heat balance for bar rolling between flat rolls in percent of the heat flux at entry to the control volume.

dr inż. Andrzej Gołdasz, agoldasz@metal.agh.edu.pl

prof. dr hab. inż. Zbigniew Malinowski, malinows@metal.agh.edu.pl

dr inż. Beata Hadała, bhadala@metal.agh.edu.pl

STADY OF HEAT BALANCE IN THE ROLLING PROCESS OF BARS

Summary

Hot rolling of shapes is one of metal forming processes that is most difficult to finite element modeling. Temperature computation is an important part of finite element software and has great influence on the solution accuracy. Computed temperature fields are generally qualitatively correct and it is not easy to eliminate wrong results. One of the possibilities to validate the temperature field is heat balance calculation in the control volume. Temperature computation is generally based on an approximate solution to the heat transport equation. Typical way of verification of the solution accuracy is to compare results of computation to measurements. However, it is not always possible or acceptable due to experimental costs. Another possibility of verification gives heat balance calculation in the control volume for separate stages of rolling. Two and three dimensional models of heat transfer in rolling processes have been tested. Stability of temperature field computation and fulfillment of heat balance have been studied for bar cooling in air and rolling between flat rolls for two sets of boundary conditions. The two dimensional model gives the temperature only in the cross section of the rolled material. Three dimensional temperature field is obtained by moving the cross section into the rolling direction. The three dimensional model uses steady solution to the heat transfer in the control volume.

Streszczenie

Istotnym elementem symulacji procesu walcowania kształtowników jest wyznaczenie pola temperatury. Uzyskiwane wyniki są trudne do weryfikacji metodami numerycznymi, pozostają drogie w zastosowaniach badania doświadczalne. Istotną podstawę do oceny dokładności rozwiązania stanowi badanie bilansu ciepła w objętości kontrolnej, którą jest fragment walcowanego pasma. Wyznaczenie pola temperatury w procesach walcowania uzyskano metodą elementów skończonych z zastosowaniem modeli dwuwymiarowych lub trójwymiarowych. Stworzone modele pozwoliły na przetestowanie dwóch schematów numerycznych: rozwiązania stacjonarnego z konwekcją oraz rozwiązania niestacjonarnego.